



ELSEVIER

Thermochimica Acta 259 (1995) 153–164

thermochimica
acta

Scanning calorimetric and EPR studies on the thermal stability of actin[☆]

Dénes Lőrinczy^{a,*}, Joseph Belágyi^b

^a Institute of Biophysics and ^b Central Research Laboratory, University Medical School,
H-7643 Pécs, Szigeti ut 12., Hungary

Received 22 July 1994; accepted 7 December 1994

Abstract

The thermal stability of actin isolated from skeletal muscle was studied in monomer and polymerized forms using DSC and EPR spectroscopy. Actin was labelled with the paramagnetic derivative of maleimide at the reactive thiol site Cys-374 in the C-terminal subdomain-1. The unfolding of actin induced by heating in the range 10–70°C resulted in a single transition: the transition temperature was $51 \pm 2^\circ\text{C}$ for G-actin, whereas $63 \pm 2^\circ\text{C}$ was obtained for the transition temperature of filamentous actin. Assuming a simple two-state transition for F-actin, the van't Hoff enthalpy was calculated to be $343.6 \pm 25.1 \text{ kJ mol}^{-1}$. The spectral changes were reversible in the temperature interval 10–65°C for F-actin, and actin did not lose its ability to polymerize.

The analysis of the DSC profiles for actin in monomer and polymerized forms enabled the assignment of three endothermic components in the F-form ($T_{m1} = 59.7 \pm 1.4^\circ\text{C}$, $H_1 = 60.3 \pm 1.7 \text{ kJ mol}^{-1}$; $T_{m2} = 60.6 \pm 1.6^\circ\text{C}$, $H_2 = 348.2 \pm 9.6 \text{ kJ mol}^{-1}$; $T_{m3} = 61.4 \pm 1.4^\circ\text{C}$, $H_3 = 104.3 \pm 4.6 \text{ kJ mol}^{-1}$), and two components in the G-form (52.5 ± 1.4 and $56 \pm 1.8^\circ\text{C}$ with enthalpies 184.4 ± 10.9 and $110.2 \pm 7.5 \text{ kJ mol}^{-1}$).

Comparison of the spectroscopic and calorimetric behavior of actin showed remarkable differences in transition temperature and enthalpy in both forms of actin, suggesting intramolecular and intermolecular interactions between subdomains and monomers that stabilize actin, especially in filament form.

Keywords: DSC; EPR; G-, F-actin; Skeletal muscle

[☆] Presented at the 13th International Symposium on Chemical Thermodynamics, Clermont-Ferrand, France, 17–22 July 1994.

* Corresponding author.

1. Introduction

It is known from earlier results that actin is found in all eukaryotic cells and is believed to play an important role in basic cellular events. In vertebrate skeletal muscle, actin is the principal component of the thin filaments, whereas in the cytoplasm of cells it is found in structures related to cell motility and transport processes [1, 2].

The contractile process is thought to depend on the interaction of proteins localized in the thick and thin filaments in striated and smooth muscle; therefore, the motional dynamics of actin and its conformation may be crucial in interaction with heavy meromyosin during the force generation of the muscle [3, 4], and the dynamical state of actin may also be important in the regulation of muscle activity [5, 6].

The thin filament dynamics and the conformation of actin can be studied by different spectroscopic methods which, in turn, reflect different types of conformational changes of the protein moiety. Fluorescence and paramagnetic probe molecules specifically attached to the Cys-374 residue of actin have proved useful in the study of actin and actin–myosin interaction [7–10]. Study of the thermal behavior and transition enthalpy gives information about the hydrophobic and electrostatic forces that stabilize the structure of the protein [11].

The aim of the present work was to investigate the thermal stability of actin and to gain information about the difference between the two forms of actin. A further intention of the present study was to attempt to compare the transition temperatures and enthalpies obtained from EPR and DSC for actin. The analysis of the experimental data suggests large differences between monomer and filamentous actins. We found that thermal stability is strongly influenced by the structural form of actin: the addition of salt that produced polymerization induced an increase in the melting temperature, and enhanced the fraction of spin labels in the strongly immobilizing state. The heating of actin led to an increase in the fraction in the weakly immobilizing state at the expense of the other population.

2. Materials and methods

2.1. Preparation and spin-labelling of actin

The isolation of actin from skeletal muscle was based on standard methods described earlier [12]. Briefly, actin was prepared from acetone-dried muscle powder by extraction at 0°C with 0.2 mM ATP, 0.1 mM CaCl₂ and 2 mM HEPES buffer (buffer A), pH 8.3, for 20 min. NaN₃ was added to the solution to a final concentration of 1 mM. The extraction was followed by two polymerization cycles. The monomer actin was polymerized by the addition of KCl to buffer A; the final concentration of KCl was 100 mM. Actin was labelled in F-form with *N*-(1-oxyl-2,2,6,6-tetramethyl-4-piperidiny)-maleimide spin label (MSL); 1.2 moles of spin label per mole of actin was reacted under continuous stirring for 90–120 min over ice. For the molecular weight of monomer actin, a value of 42 kD was assumed. The unreacted labels were removed by pelleting the actin by ultracentrifugation. The pellet was gently homogenized with

a teflon homogenizer in buffer A. The homogenizate was exhaustively dialysed overnight against the extraction solution at 4°C. The EPR measurements were performed on samples in the concentration range of 50–100 μM . The concentration was determined by measuring the optical absorption with a Hitachi 124 spectrophotometer. The absorbance of the monomer actin was taken as $E^{280}(0.1\%) = 0.63$.

2.2. Electron paramagnetic resonance (EPR) experiments

The EPR measurements were made with ERS 220 (Center of Scientific Instruments, Germany) and ESP 300 E (Bruker, Germany) X-band spectrometers. For the conventional EPR technique, 100 kHz field modulation (0.1–0.25 mT amplitude) and 2–20 mW microwave power were used. The measurements were made in the temperature range of 10–70°C with an accuracy of $\pm 1^\circ\text{C}$.

Signals due to EPR absorption were detected in rapid scan mode by a microcomputer system interfaced to the ERS 220 spectrometer. The derivatives of the EPR absorption spectra were digitized into 1024 data points at equal intervals over a 10-mT sweep width of the magnetic field and stored on discettes. The digitized spectra were normalized to the same number of unpaired electrons by taking into account the double integral of the derivative spectra. The calibration of the spin concentration was made with a known concentration of maleimide spin label solution using the same sample cell as for the actin solution. The spectra of the protein samples were characterized with the hyperfine splitting constant and the intensity ratio of the first two low-field peaks.

2.3. Differential scanning calorimetry

DSC measurements were performed with a Setaram Micro DSC II calorimeter. The experiments were done in the 10–90°C temperature range with a 0.3 K min^{-1} scanning rate. Standard “batch” Hastelloy cells were used with an average 850 μl sample volume. The conventional actin buffer (buffer A) was used as reference.

2.4. Viscosity measurements

Viscosity measurements were performed using Ubbelohde viscometers supplied with a thermostated waterbath at $22 \pm 0.3^\circ\text{C}$. The outflow times for about 1 ml of water were 40 or 130 s.

3. Results and discussion

3.1 Rotational motion of spin labels in actin

The conventional EPR spectrum of actin in monomer form could be interpreted as a superposition of spectra arising from labels which were bound to strongly and weakly immobilizing sites [10]. The amount of labels attached to weakly immobilizing sites

was not more than 5–7% of the total absorption. It is known from earlier experiments that Cys-374 incorporated more than 90% of the labels under the conditions used in our experiments, evidencing that the labelling procedure was highly selective. Upon polymerization to F-actin, the EPR spectrum revealed an increased immobilization of the strongly immobilizing sites. The hyperfine splitting constant changed from $2A'_{zz} = (6.328 \pm 0.05) \text{ mT}$ ($n = 16$) to $(6.780 \pm 0.02) \text{ mT}$ ($n = 7$) after one hour of polymerization at room temperature. These results agree quite well with the earlier observations [7,8,13,14]. From the spectral parameters, it could be deduced that the labels were rigidly attached to the actin monomers and they indicated the motion of a larger domain. In polymerized form, the rotational motion of the labels, as seen by the saturation transfer EPR spectroscopy (not shown), most probably reflected the torsional motion of several associated subunits [2,7,15].

3.2. Thermal treatment of actin

The experimental results are summarized in Figs. 1, 2 and 3. A typical room-temperature spectrum of maleimide labels attached to monomer actin is shown in Fig. 1, Curve B. At 48°C (Fig. 1), the spin labels on G-actin have a greater degree of

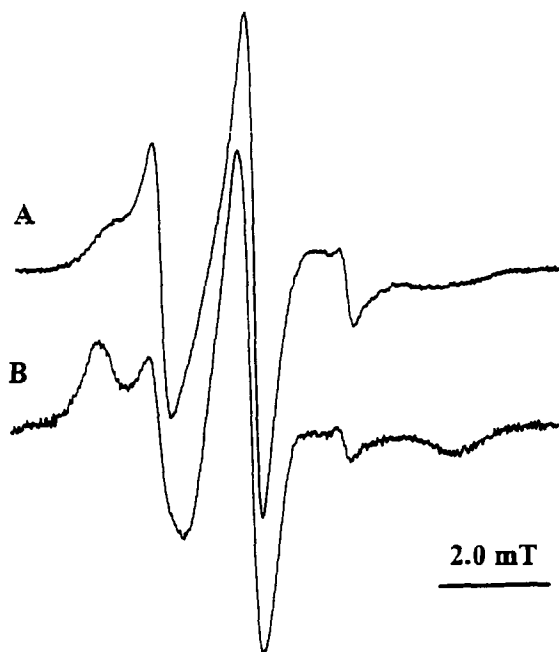


Fig. 1. EPR spectra of skeletal muscle G-actin labelled with maleimide-based spin label at the Cys-374 residue at different temperatures. The concentration of actin was 2.6 mg ml^{-1} . A: 48°C; B: 20°C. The temperature was increased from 10°C up to 48°C in 10°C steps, and the measurement was made after 10 min heating.

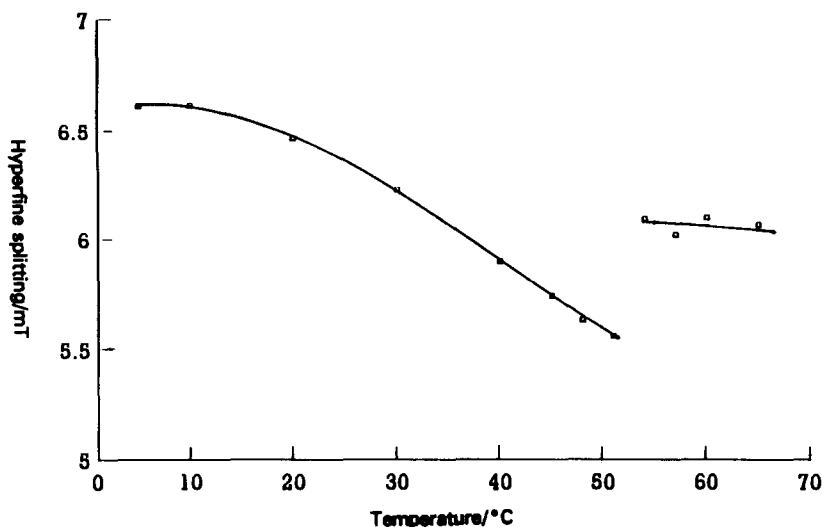


Fig. 2. Temperature dependence of $2A'_{zz}$ for spin-labelled G-actin. The hyperfine splitting values were obtained by increasing the temperature from 10°C up to 65°C.

rotational freedom. Similar spectral changes were detected on F-actin samples. The changes upon thermal treatment in the rigidity of the protein structure can be seen in Figs. 2 and 3, where the hyperfine splitting parameter $2A'_{zz}$ of the labels is plotted against temperature.

The experiments showed that

(i) The lineshape of the spectrum for G-actin changed rapidly with increasing temperature; the contribution of strongly immobilized labels to the total EPR absorption was very small at about 51°C, implying the unfolding of the environment of the labelled sites. This temperature might correspond to the transition temperature for monomer actin; $T_m = 51^\circ\text{C}$. At 54°C, a new spectral component could be detected; its splitting constant was comparable to F-actin. It is very likely that this component arises from aggregated actin monomers.

(ii) The parameter $2A'_{zz}$ for F-actin decreased similarly with increasing temperature. At about 60°C an abrupt decrease in $2A'_{zz}$ was detected which could not be explained by a fall in viscosity. This might characterize the thermal unfolding of the protein; we calculated $63 \pm 2^\circ\text{C}$ for the transition temperature T_m , suggesting a single transition.

(iii) The thermal treatment was followed by an increase of the mobile component at the expense of the component arising from strongly immobilized labels; the conformational transition induced by thermal treatment was reversible in the environment of the labelled sites until 48°C in the case of monomer actin, and until 65°C in the case of polymerized actin.

(iv) The spin label spectra which were sensitive to the polymerization of actin exhibited that the F → G and G → F transitions could be accomplished at 4°C on F-actin thermally treated for 10 min at a temperature not higher than 60°C [14].

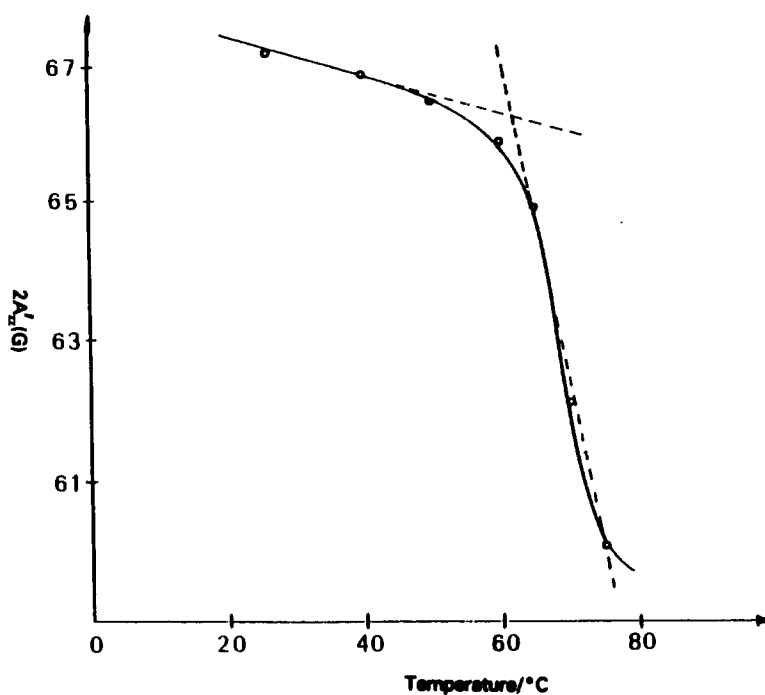
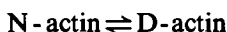


Fig. 3. Temperature dependence of $2A'_{zz}$ for spin-labelled F-actin. Actin was polymerized by addition of KCl and $MgCl_2$; the final concentrations were 100 mM and 2 mM, respectively. The measurement of the F-actin sample was performed after one hour polymerization. The hyperfine splitting values were obtained from spectra taken at increasing temperatures.

It was of interest to further characterize actin upon thermal treatment. The relative viscosity of actin in the F-form showed similar thermal behaviour. The samples were heated for 10 min at the selected temperature; thereafter they were cooled down to room temperature and viscosity measurements were performed. The relative viscosity did not change upon heating until 60°C, and we obtained the same value, within the limits of experimental error, as on untreated samples. In contrast, treatment at higher temperatures produced a significant decrease in the relative viscosity. The large change is probably due to partial depolymerization of F-actin or the breaking of the filaments induced by thermal treatment.

3.3. Calculation of thermodynamic parameters

Analysis of EPR spectra revealed one transition. In order to determine the thermodynamic parameters of actin denaturation using EPR data, we assumed that the thermal denaturation was a two-state process without stable intermediates



where N and D denote the native and denatured state, respectively. It was also assumed that the fraction of strongly immobilized labels represented the N-actin state of the sample. The increase in temperature produced continuously increasing thermal fluctuations and led to a decrease in the contribution of strongly immobilized labels to the entire spectrum, thus allowing the calculation of the equilibrium constant at each temperature (Table 1). Under these conditions the equilibrium constant showed a slight temperature dependence (Fig. 4). For the purpose of calculation of the van't Hoff enthalpy, we assumed that the linearity held in the temperature range of 60–70°C. The ΔH associated with the thermal denaturation of F-actin was determined to be $343.6 \pm 25.1 \text{ kJ mol}^{-1}$, which is considerable smaller than the calorimetric enthalpy ($548.9 \pm 12.6 \text{ kJ mol}^{-1}$).

3.4. Calorimetric measurements

In Figs. 5 and 6, typical DSC profiles for G- and F-actin are shown. The major transition in F-actin was obtained with a T_m of $61 \pm 2^\circ\text{C}$ at pH 8.3. Our data are smaller than those reported earlier [16]. The average denaturation temperature range was 54–64°C which broadened as the pH of the protein solution became lower (at pH 6.4, ΔT was 55–68°C). The total calorimetric enthalpy change was estimated to be $548.9 \pm 25.1 \text{ kJ mol}^{-1}$ at pH 8.3 which could be decomposed into three different transitions ($T_{m1} = 59.7 \pm 1.4^\circ\text{C}$, $H_1 = 60.3 \pm 1.7 \text{ kJ mol}^{-1}$; $T_{m2} = 60.6 \pm 1.6^\circ\text{C}$, $H_2 = 348.2 \pm 9.6 \text{ kJ mol}^{-1}$; $T_{m3} = 61.4 \pm 1.4^\circ\text{C}$, $H_3 = 104.3 \pm 4.6 \text{ kJ mol}^{-1}$). In contrast, for monomer actin we had a T_m of $51 \pm 1.5^\circ\text{C}$ at pH 8.3. The net calorimetric enthalpy change was $297.5 \pm 16.8 \text{ kJ mol}^{-1}$ and we found two transitions at temperatures of

Table 1
Thermal denaturation of skeletal actin^a

$T/^\circ\text{C}$	$10^3/T$	x	K	$\ln K$
60.0	3.003	0.0630	0.0673	-2.6980
62.5	2.9806	0.1144	0.1292	-2.0460
65.0	2.9580	0.2162	0.2758	-1.2887
67.5	2.9368	0.4054	0.6818	-0.3829
68.7	2.9260	0.5495	1.2200	0.1988 ^b
70.0	2.9150	0.6756	2.0833	0.7339
72.5	2.8940	0.8558	5.9375	1.7812

^a Actin prepared from rabbit skeletal muscle was spin-labelled in F-form with maleimide-based paramagnetic probe molecules for 90 min at 0°C. Unreacted labels were removed by pelleting the actin sample, and the pellet was dialyzed overnight against G-buffer at 4°C after homo-genizing. Actin was centrifuged with $100\,000 \times G$ and polymerized in F-buffer. The samples were heated at increasing temperature for 10 min and spectra were taken at the selected temperature. In the table the fraction of the denatured actin is denoted by x .

^b Extrapolated value.

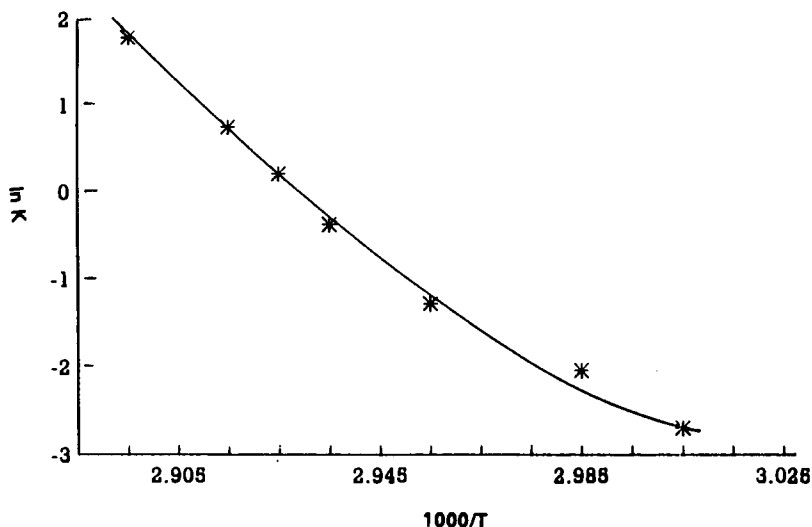


Fig. 4. Temperature dependence of the equilibrium constant calculated from the EPR spectra of F-actin at different temperatures. Data of the measurements are included in Table 1.

52.5 ± 1.4 and $56 \pm 1.8^\circ\text{C}$ with enthalpies 184.4 ± 10.9 and $110.2 \pm 7.5 \text{ kJ mol}^{-1}$, respectively. A similar value was obtained for cardiac G-actin using circular dichroism [17]. It is interesting to note that the calorimetric enthalpy of the main transition agrees well with the van't Hoff enthalpy calculated from the EPR data. This suggests that the main transition represents the thermal denaturation of subdomain-1 (or domain 1), and supports the assumption about the thermal transition of at least two independent domains based on our calorimetric data.

3.5. Relationship between actin structure and thermal stability

Electron microscopic and spectroscopic data suggest strong correlation between structural disorder and the flexibility of actin. Considering the atomic model of the F-actin filaments, it was assumed that the intersubunit contact between the subunits along the filament is much stronger than the interaction between the subunits of the two long-pitch helical strands, and this might result in 2–6-subunit-long stretches in which the genetic helix is loosened [19, 20]. Thus, F-actin filaments may locally deviate significantly from a perfect helical structure. We can assume that the number of these helical stretches increases with increasing temperature; therefore these structural deviations may also contribute to the increased torsional flexibility of the filaments.

Analysis of the thermal stability of the proteins indicates that the heat capacity profiles of most of the proteins are complex and they reflect the stabilizing forces acting in the protein structure between amino acid side chains and/or protein segments or domains [17]. In contrast, the spectroscopic data give information about the environment of the reporter group. The maleimide labels are rigidly attached to Cys-374;

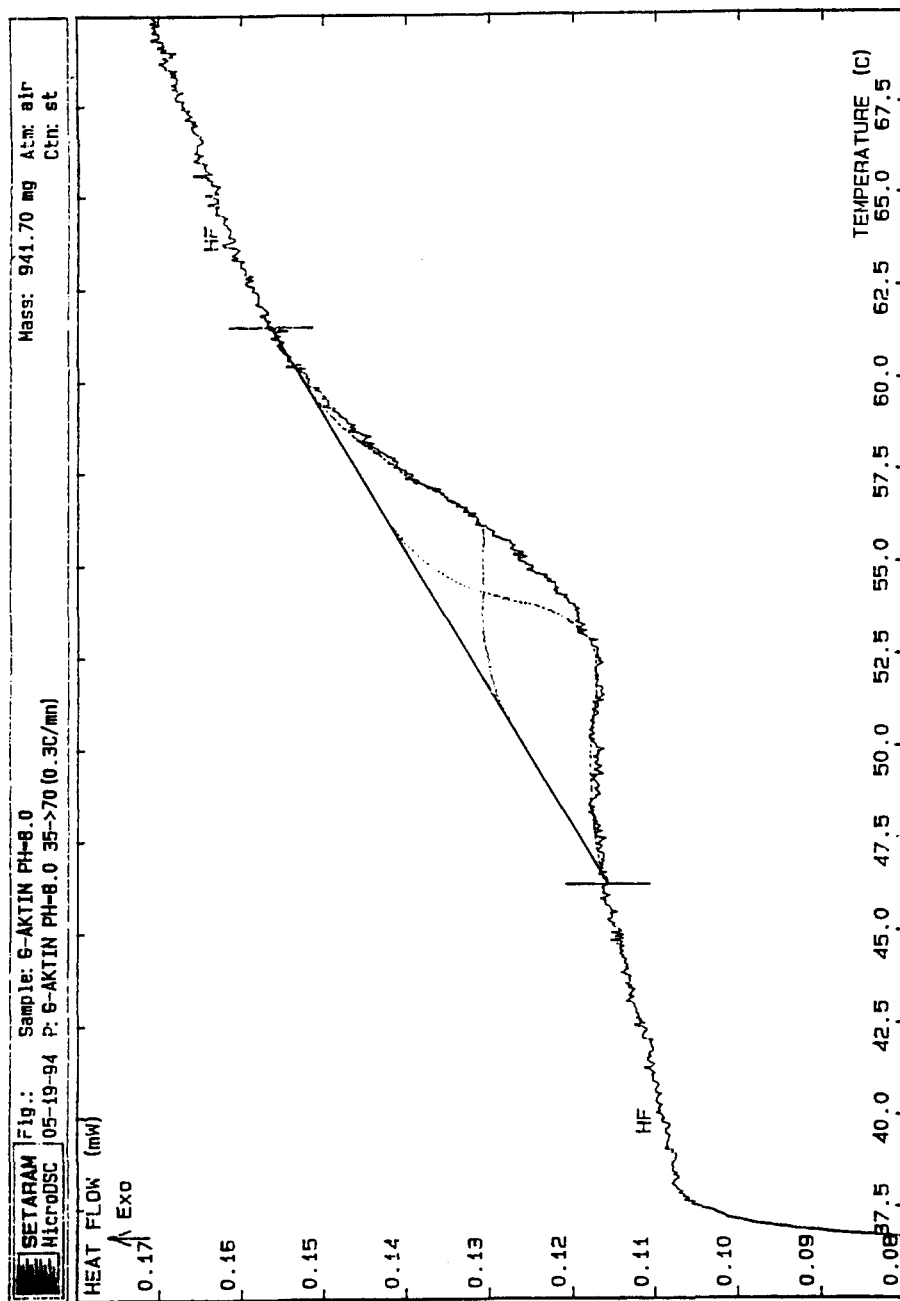


Fig. 5. Temperature dependence of heat flow of G-actin in the range 40–65°C, together with decomposition of the DSC scan. The concentration of actin was 2.38 mg ml⁻¹ in buffer A.

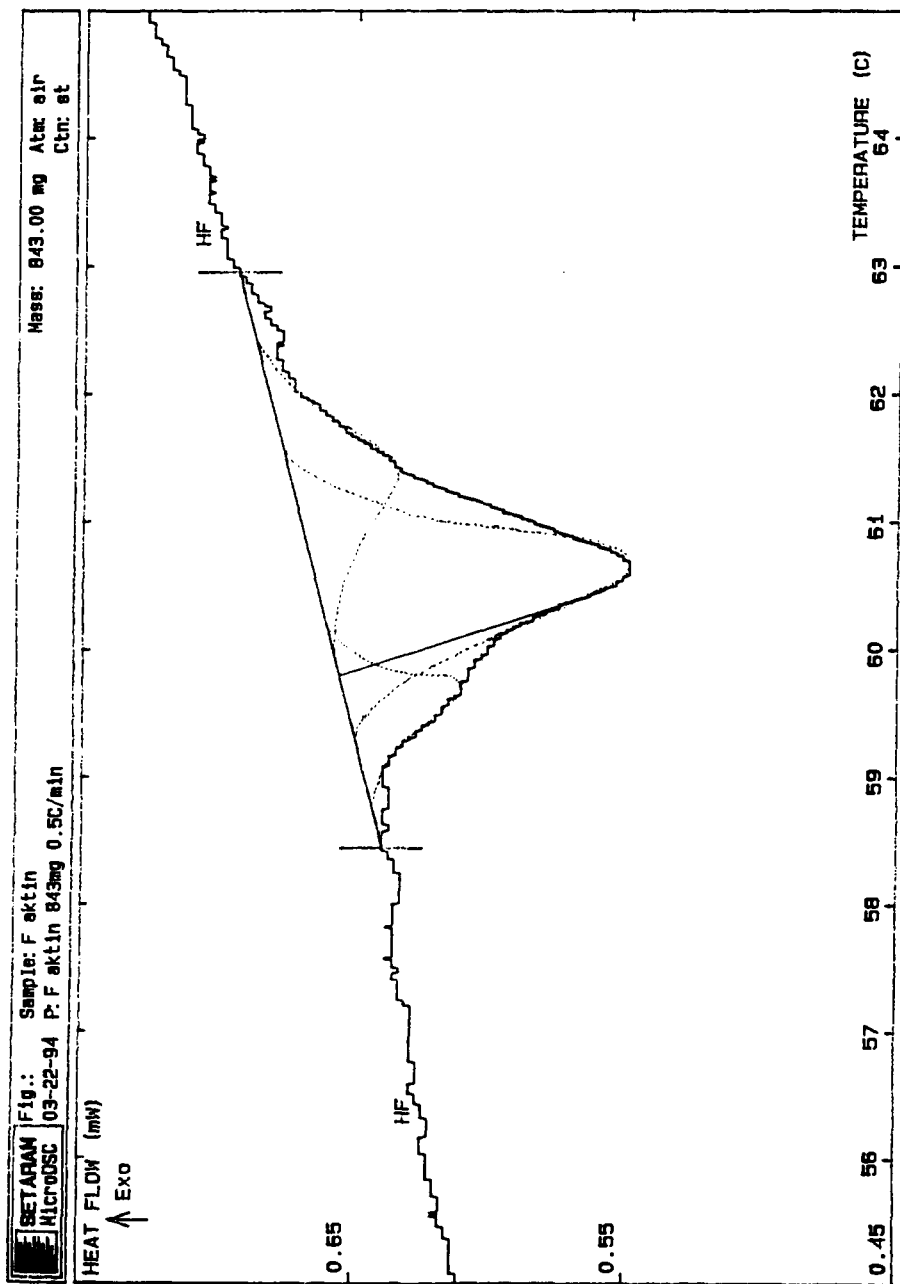


Fig. 6. The endothermic melting of F-actin (1.6 mg ml^{-1}) including the possible deconvolution of the experimental data. Polymerization was induced by addition of 100 mM KCl .

therefore they reflect the flexibility of subdomain-1. The polymerization of actin was accompanied by a significant increase in T_m and ΔH , implying that the monomer–monomer interaction enhances the thermal stability [16]. The fact that the EPR results reflected similar changes in the thermodynamic parameters supports the view that the internal structure of subdomain-1 might become more compact upon polymerization. It is known that actin monomers consist of structural domains which are separated by a cleft, and the bound nucleotide is localized in the cleft [21–23]. We cannot exclude that the binding of actin monomers to another actin monomer affects the conformation of the segment that holds the labels and this allows a conformational conversion for the bound nucleotide which is accompanied by change in the orientation and/or mobility of the labels. It was shown recently that the binding of subfragment-1 to actin in ghost muscle fibres induced changes in the domain orientation of actin [24]. The process might be modulated by the altered interaction between the subunits of the two long-pitch helical strands.

Since we have several unknown points in the properties of the actin assemblies, further experiments are needed to discover the details of actin's flexibility and its special interactions in biological functions.

Acknowledgements

This work was supported by research grants from the Hungarian Scientific Research Foundation (OTKA No. CO-272 and No. 2044) and Ministry of Health (T-06 737/93). The complete IBM PC 386 DX configuration was supported by POPEX Ltd., Pécs, Hungary.

References

- [1] E. Lazarides and J.P. Revel, *Sci. Am.*, 240 (1979) 88–100.
- [2] K. Mihashi, M. Yoshimura and T. Nishio, in C.G. Dos Remedios and J.A. Barden (Eds.), *Actin: Structure and Function in Muscle and Non-Muscle Cells*, Academic Press, Sydney, (1983), pp. 81–88.
- [3] H.E. Huxley, *Science*, 164 (1969) 1356–1366.
- [4] A.F. Huxley and R. Simmons, *Nature*, 233 (1971) 533–538.
- [5] R.C. Craig, E. Szent-Györgyi, L.G. Beese, P. Flicker, P. Vigert and C. Cohen, *J. Mol. Biol.*, 140 (1980) 35–36.
- [6] S. Fujime and S. Ishiwata, *J. Mol. Biol.*, 62 (1971) 251–265.
- [7] D.D. Thomas, J.C. Seidel and J. Gergely, *J. Mol. Biol.*, 132 (1979) 257–273.
- [8] O.D. Harwell, M.L. Sweeney and F.H. Kirkpatrick, *J. Biol. Chem.*, 255 (1980) 1210–1220.
- [9] M. Miki, P. Wahl and J.C. Auchet, *Biochemistry*, 21 (1982) 3661–3665.
- [10] M. Mossakowska, J. Belágyi and H. Strzelecka-Golaszewska, *Eur. J. Biochem.*, 175 (1988) 557–564.
- [11] C. Tanford, *Adv. Protein Chem.*, 23 (1968) 121–275.
- [12] J.A. Spudich and S. Watt, *J. Biol. Chem.*, 246 (1971) 4866–4871.
- [13] R. Cooke and M. Morales, *J. Mol. Biol.*, 60 (1971) 249–261.
- [14] J. Belágyi, P. Gróf and G. Pallai, *Acta Biochim. Biophys.*, 14 (1979) 293–296.
- [15] M.D. Barkley and B.H. Zimm, *J. Chem. Phys.*, 70 (1979) 2991–3007.
- [16] A. Bertazzon, G.H. Tian, A. Lamblin and T.Y. Tsong, *Biochemistry*, 29 (1990) 291–298.
- [17] C.C. Contaxis, C.C. Bigelow and C.G. Zarkadas, *Can. J. Biochem.*, 55 (1977) 325–331.

- [18] D.L. Stokes and D.J. DeRosier, *J. Cell Biol.*, 104 (1987) 1005–1017.
- [19] A. Bremer, R.C. Millonig, R. Sütterlin, A. Engel and T.P. Pollard, *J. Cell Biol.*, 115 (1991) 689–703.
- [20] H.P. Erickson, *J. Mol. Biol.*, 206 (1989) 465–474.
- [21] W. Kabsch, H.G. Mannherz and D. Suck, *EMBO J.*, 4 (1985) 2113–2118.
- [22] J.A. Barden, *Biochemistry*, 26 (1987) 6023–6030.
- [23] W. Kabsch, H.G. Mannherz, D. Suck, E. Pai and K.C. Holmes, *Nature*, 347 (1990) 37–44.
- [24] Y.S. Borovikov and V.P. Kirilina, *Tsitologia*, 33 (1992) 68–75.